Cell and Tissue Research (2024) 395:117–131
https://doi.org/10.1007/s00441-023-03848-5

REGULAR ARTICLE

A new technology for the treatment of premature ovarian insufficiency: Cell sheet

Pinar Calis[1,2] · Gokcenur Arik[2] · Cemile Merve Seymen[2] · Gokce Kaynak Bayrak[3] · Ozge Ekin Akdere[4] · Canan Yilmaz[5] · Atiye Seda Yar Saglam[6] · Menemşe Gümüşderelioğlu[7] · Gulnur Take Kaplanoglu[2]

Received: 7 April 2023 / Accepted: 22 November 2023 / Published online: 5 December 2023
© The Author(s), under exclusive licence to Springer-Verlag GmbH Germany, part of Springer Nature 2023

Abstract

Premature ovarian insufficiency (POI) is defined as the development of hypergonadotropic hypogonadism before the age of 40 with definitive treatment being absent. In the current study, we aim to compare the efficacy of the cell sheet method with an intravenous (IV) application of adipose-derived mesenchymal stem cells (AdMSCs) to the POI with an animal model. In the current prospective study, 6-to-8-week-old Sprague Dawley rats were generated four groups: (i) a control group in which only PBS was administered; (ii) an only-POI group generated by cyclophosphamide; (iii) a POI group treated by way of IV AdMSCs; and (iv) a POI group treated by way of the cell sheet method. Twenty-eight days after an oophorectomy was performed, intracardiac blood was taken. Follicle count, immunohistochemical examination for GDF9, BMP15, and TUNEL were conducted, gene expressions of GDF9 and BMP15 were examined, and E2 was measured in the serum samples. With hematoxylin-eosin, in the third group, multi oocytes follicles were the most remarkable finding. In the fourth group, most of the follicles presented normal morphology. GDF9 involvement was similar between the first and fourth groups. BMP-15 immunoreactivity, in contrast to fourth group, was weak in all stages in the second and third groups. The current attempt represents a pioneer study in the literature in which a cell sheet method is used for the first time in a POI model. These results suggest that the cell sheet method may be a feasible and efficient method for the stem cell treatment of models with POI and could be a new treatment approach in POI.

Keywords Premature ovarian insufficiency · Stem cell · Cell sheet · GDF9 · BMP15

Introduction

Premature ovarian insufficiency (POI) is a major health issue defined as the partial or total loss of the reproductive function of the ovaries under the age of 40 due to follicular disfunction or early follicular loss (Martin et al. 2017; Nelson 2009). Although the incidence is 1 in 100 by the age of 40, an increasing number of younger women face this condition with various menopausal-like symptoms, such as vaginal dryness, hot flushes, and irregular or absent menstruation. In recent years, due to a significant increase in the childbearing age, infertility has become the major problem of POI. On the other hand, because of a diminished ovarian reserve in POI, routine infertility treatment (such as assisted reproductive techniques (ART)) does not offer promising results for these patients.

In recent years, there have been several encouraging studies for the treatment of infertility in POI patients.

✉ Pinar Calis
ptokdemir86@gmail.com

1 Department of Obstetrics and Gynecology, Gazi University Faculty of Medicine, Ankara 06100, Turkey

2 Department of Histology and Embryology, Gazi University Faculty of Medicine, Ankara, Turkey

3 Department of Biomedical Engineering, Izmir Bakircay University, Izmir, Turkey

4 Department of Bioengineering, Hacettepe University, Ankara, Turkey

5 Department of Biochemistry, Gazi University Faculty of Medicine, Ankara, Turkey

6 Department of Medical Biology and Genetics, Gazi University Faculty of Medicine, Ankara, Turkey

7 Department of Chemical Engineering, Hacettepe University, Ankara, Turkey

The introduction of in vitro activation (IVA) (Kawamura et al. 2016), using PI3K/Akt/mTOR and Hippo signaling pathways, was a new insight for POI patients. Although the preliminary results demonstrate high pregnancy and live birth rates, the following studies by different groups suggest that both pregnancy and live birth rates are comparable with POI patients not receiving any treatment (Diaz-Garcia et al. 2022). Apart from IVA, there have been recent studies proposing the administration of stem cells, which may give new hope for the treatment of POI patients by means of fertility. The initial results in animal studies are promising for follicular development in POI rats (Wang et al. 2013). In addition to this, follicular stimulating hormone (FSH), anti mullerian hormone (AMH), and estradiol (E2) were restored after stem cell treatment (Li et al. 2017). Stem cells were administered mostly intravenously (IV) or by way of the intraovarian route by direct administration (Zhang et al. 2017). On the other hand, these methods have several drawbacks, such as systemic effects of stem cells not being known for the IV method and possible trauma to the ovary for the intraovarian method.

Cell sheet technology is a relatively new tissue engineering technique first used by Shimizu et al. (2003). This technique allows cells to separate from a culture dish without using a chemical, toxin, or a proteolytic enzyme. Therefore, the connections between cells are not disrupted and the extracellular matrix (ECM) is preserved. In this way, cells sensitive to damage due to certain toxins, such as hepatocytes and glial cells, are not damaged (Chen et al. 2015). The first application of the technique was based on the use of temperature sensitive culture dishes. Based on this, below 32 °C, cells can be obtained in layers in less than 30 min without the use of enzymes or chelating agents. The cell sheet technique has several advantages in regenerative medicine. Other than preserving cellular microenvironment, such as ECM, ion channels, cell surface proteins, and growth factor proteins, there is minimal cell loss when compared to the conventional direct cell suspension injection technique. Studies show that, compared to cell suspension injection, cell sheet transplantation provides stronger tissue function, more potent tissue regeneration and a more powerful therapeutic effect (Chen et al. 2015; Owaki et al. 2014).

From this, in the current study, our aim is to compare ovarian regeneration by immunohistochemical and genetic analysis in cyclophosphamide induced POI models using rats by administration of adipose-derived mesenchymal stem cells by way of the IV and cell sheet methods.

Materials and methods

In vitro studies

Production of cell sheets

The ascorbic acid treatment method was used to produce adipose-derived mesenchymal stem cell (AdMSCs) sheets (Yilmaz et al. 2023). The cells were isolated from the adipose tissue of adult rats (Hacettepe University Animal Experimentations Ethics Board. Decision No. 2015/32). The isolation procedure and characterization of the cells were explained in our previous study (Akdere et al. 2019). Briefly, cell viability and proliferation were determined using PrestoBlue analysis, cell morphology was investigated using immunofluorescent staining of F-actin and nucleus. Also, cells were analyzed for MSCs specific markers using fluorescence-activated cell sorting. In addition, osteogenic, adipogenic, and chondrogenic differentiation of AdMSCs were demonstrated. In order to produce cell sheet, cells at passage 3–4 were seeded into 12-well culture dishes at a density of 5×10^4 cells/cm^2. The next day, the culture medium was replaced with medium containing 100 µg/mL L-ascorbic acid 2-phosphate (AA2P, Cayman Chem., USA) to promote the sheet formation of the cells and the culture was continued to reach confluency. On the fourth day of the culture, the cell sheets were peeled off from the surface by gently washing with Dulbecco's phosphate buffer solution (DPBS) and transferred to new 12-well culture dishes using a simple pipetting technique (Kaynak Bayrak and Gumusderelioglu 2019).

Characterization of the cell sheets

Live/dead cell staining, immunofluorescence staining and scanning electron microscopy (SEM) analyzes were performed within the scope of the characterization studies of the produced cell sheets.

Immunofluorescent staining

The obtained cell sheets were washed twice with a phosphate buffer solution (PBS) and fixed with 4% (w/v) paraformaldehyde at room temperature for 30 min. After washing three times with PBS, the cell membrane permeability was increased by treating with 0.1% (v/v) Triton X-100 (in PBS) for 10 min and washed three times with 1% (w/v) bovine serum albumin (BSA) solution (in PBS; PBS-A). Subsequently, the samples were incubated in 1% (v/v) Alexa Fluor

488 Phalloidin conjugated anti-F-actin antibody and 0.1% (v/v) DAPI containing PBS-A solution at room temperature and blocked from light exposure for 30 min. After this, the antibody solution was removed, and the cells were washed three times with PBS-A and visualized with a fluorescent microscope (Olympus XI71, USA) to observe the cytoskeletal orientation of the cells.

Live/dead cell staining

The viability of the stem cells before detachment was investigated with live/dead cell staining by using Ethidium homodimer-1 and calcein-AM stains. The samples were then washed with PBS and visualized using a fluorescent microscope.

Scanning electron microscopy (SEM) analysis

Morphological observation of the cell sheets was performed by SEM analysis. The samples were washed with DPBS and fixed with 2.5% (v/v) glutaraldehyde solution for 30 min. After this, the cell sheets were washed three times with PBS and stored in 1% P/S containing PBS at 4 °C until analysis. The dehydration procedure was performed through a graded ethanol series (10%, 30%, 50%, 70%, 90%, and 100% v/v, respectively) and kept in hexamethyldisilazane (HMDS) for 5 min, 1 day before the observation. After this, the samples were dried in a fume hood overnight. Before the analysis, the samples were coated with gold-palladium and observed under an SEM analysis (Tescan, GAIA 3, Czech Republic).

Preparation of cell sheets for transplantation

The cells were labeled with 5-bromo-2′-deoxyuridine (BrdU, BD Pharmingen, San Jose, CA) on the third day of cell sheet production to track the cells after transplantation. After the cells were incubated with BrdU for 3 h at 37 °C, they were washed with DPBS and cultivated in a growth medium.

On the day of transplantation, the cell sheets were removed from the surface with PBS washing and transferred to a new sterile 6-well culture dish. After carefully uncovering the mouse ovaries, a support membrane was used for transplantation of the cell sheets onto the ovary. The polyvinylidene fluoride (PVDF) membrane filter (Durapore®, Merck) was cut to cover the cell sheets, and the middle part of the membrane was also cut, leaving the cell sheets free. Therefore, the transport membrane was obtained in the form of a ring for easy separation of the cell sheets from the membrane (Fig. 1). The support membrane was carefully placed on the detached cell sheet and left for a short time to allow the cells to adhere to the membrane. After this, the membrane was carefully lifted using forceps and the cell sheet was placed on the ovary. Because the PVDF membrane was only a transport membrane, it was not left on the ovary. There was a hole in the middle part of the membrane, and after the cell sheet adhered on the ovarian surface, the PVDF membrane was separated from the cell sheet.

In vivo studies

Animal model and surgical procedures

A total of 40 female fertile adult *Sprague Dawley* rats, 6–8 weeks old, were used. All the animals were obtained from the Gazi University Animal Research Center and kept at a standardized temperature and humidity environment on a 12-h day/night cycle and were fed ad libitum. All the experimental procedures were performed following the approval of the Gazi University Ethical Committee on Animal Research (Approval No: 21/12/2018-E.168939).

The rats were divided into four groups: Group I ($n = 10$) was the control group (PBS injection, without stem cell treatment); Group II ($n = 10$) was the POI group (200 mg/kg cyclophosphamide (CTX), intraperitoneally (IP), single dose) (Endoxan-Eczacibasi Baxter, Turkey, with PBS); Group III ($n = 10$) was the POI (200 mg/kg CTX, IP, single dose) + AdMSCs (4×10^5 stem cells) via IV (tail vein); and Group IV ($n = 10$) was the POI (200 mg/kg CTX, IP, single dose) + AdMSCs (4×10^5 stem cells) by way of cell sheet (only to right ovary). To prove formation of the POI model, one rat from each group was sacrificed after CTX application (Bao et al. 2018) (Fig. 2).

Surgery was performed after anesthesia with intraperitoneal administration of ketamine hydrochloride (50 mg/kg Ketalar; Eczacibasi, Istanbul, Turkey) and xylazine hydrochloride (10 mg/kg Rompun; Bayer Turk Ilac Ltd, Istanbul, Turkey). After cleaning the operation site with an antiseptic solution (Baticon; Drogsan, Turkey), laparotomies were performed by way of a 25 mm midline-vertical incision. For groups I, II, and III, only a laparotomy was performed; for Group IV, after a laparotomy, an AdMSCs sheet was applied to the right ovary (Fig. 3). Twenty-eight days after surgery (Bao et al. 2018), the rats were sacrificed by high dose anesthetic application. Blood samples were obtained by way of intracardiac injection for E2 levels, and right oophorectomy was performed for histologic and genetic analysis.

BrdU staining method

To show BrdU positive cells in tissues in the experimental groups, a BrdU in-situ detection kit (BD Pharmingen, San Jose, CA) was used. Imaging was carried out using a Leica DCM 4000 (Germany) light microscope and an LAS program.

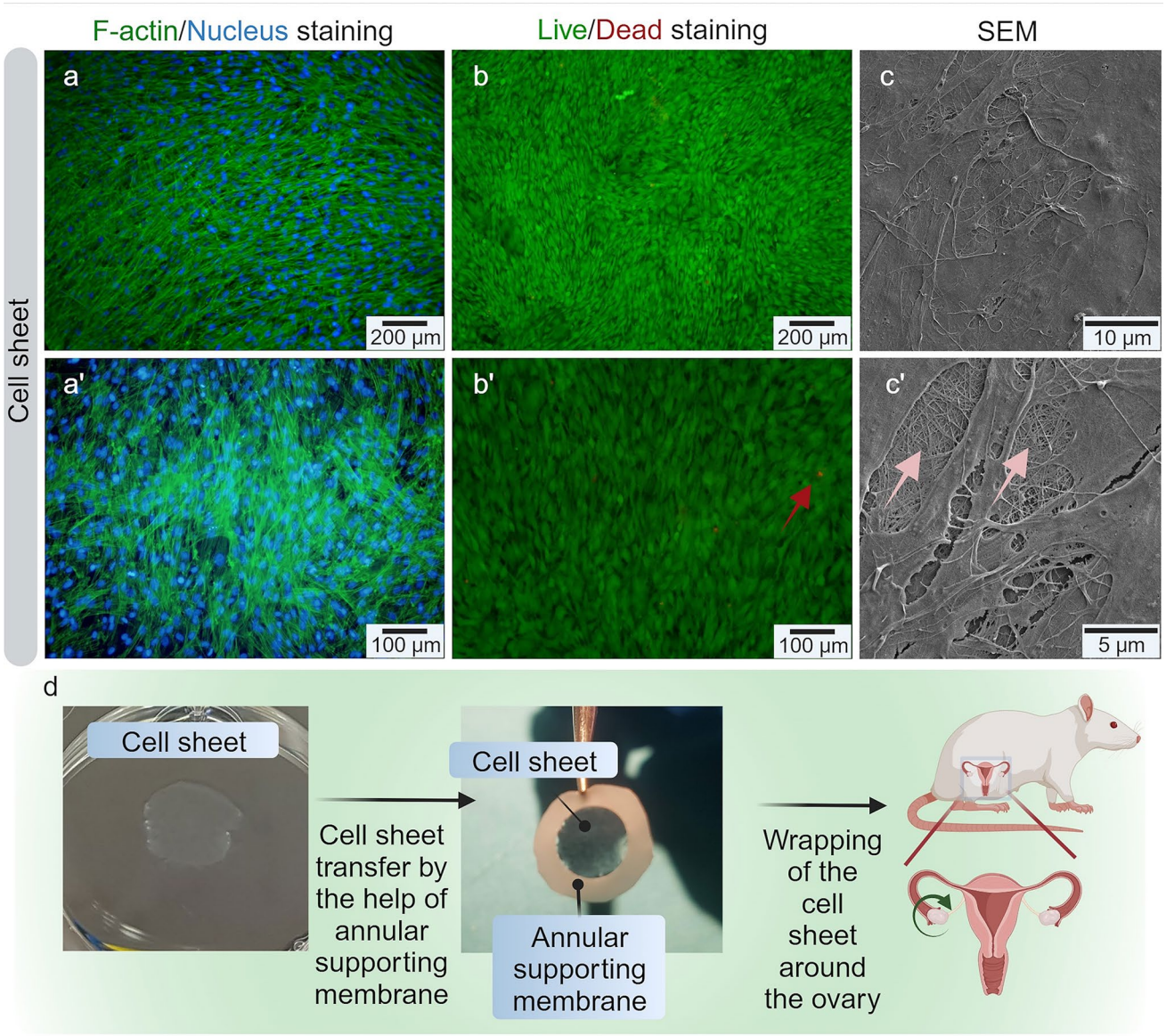


Fig. 1 **a** Immunofluorescence staining photographs of AdMSCs sheets (20×, scale bar 100 µm). **a′** Immunofluorescence staining photographs of AdMSCs sheets (40×, scale bar 50 µm). **b** Live/dead cell staining photographs (10×, scale bar 200 µm). **b′** Live/dead cell staining photographs (20×, scale bar 100 µm) with dead cell nuclei shown by a red arrow. **c** SEM photographs (4000×, scale bar 10 µm. **c′** SEM photographs (10,000× scale bar 5 µm), fiber structures within intense ECM are shown by arrows. **d** Schematic representation of the in vivo transplantation of cell sheets

Hematoxylin-eosin staining

Ovarian samples were fixed in 4% neutral formaldehyde for 72 h. After washing in tap water, the samples were dehydrated through ascending alcohols and cleared in xylene, then they were embedded in paraffin. Cross sections were cut at 4 µm using a microtome and mounted on poly-L-lysine-coated slides. Hematoxylin-eosin was then performed on 4 µm thick sections. The sections were evaluated using a light microscope equipped with a digital camera (DM4000B Image Analyze System; Leica, Wetzlar, Germany), a Leica DFC280 plus camera, and an LAS software program (Leica).

Immuno-histochemical analysis

The immuno-histochemical procedure explained in our previous study was administrated with our 4 µm ovary cross sections. The dilutions and times of primary antibodies against GDF-9 were: (Bioss, 100 µl Rabbit Polyclonal Antibody, ref:bs-3759R, lot:980691W, USA); 1:100 [with PBS]; overnight at +4 °C), BMP-15 (Bioss, 100 µl Rabbit

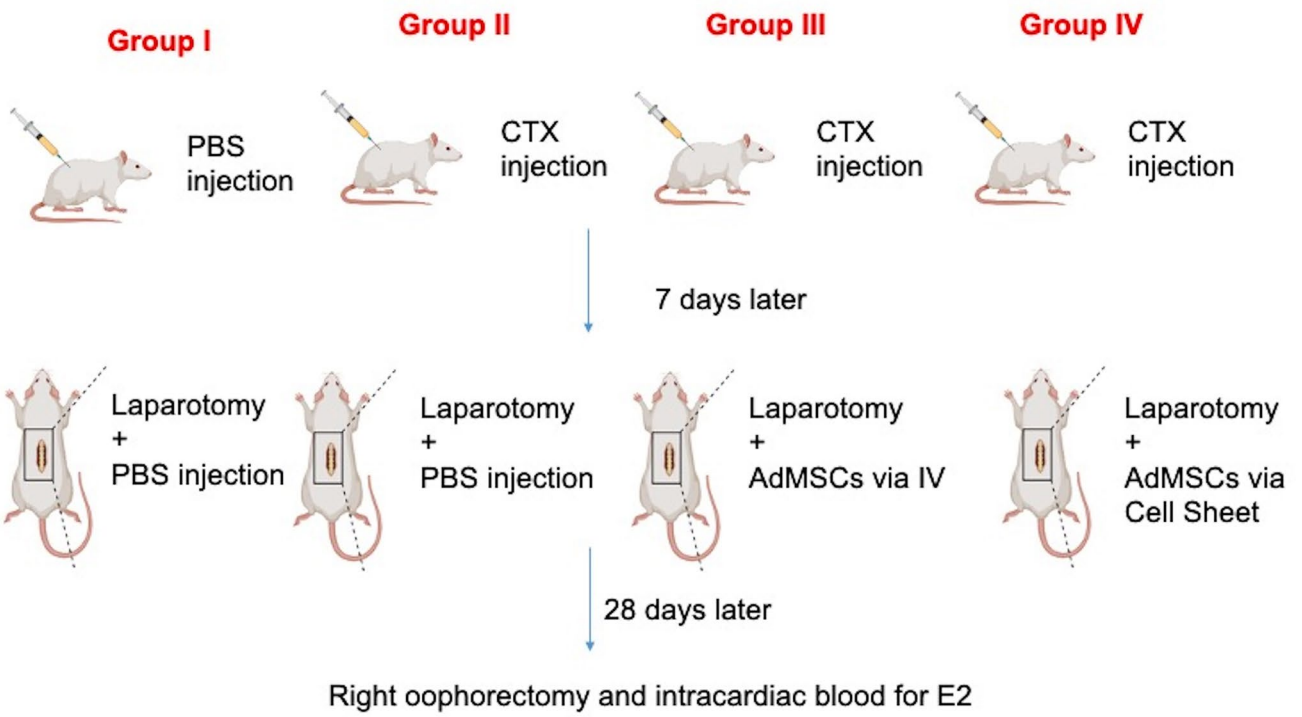


Fig. 2 Timeline of the experimental model

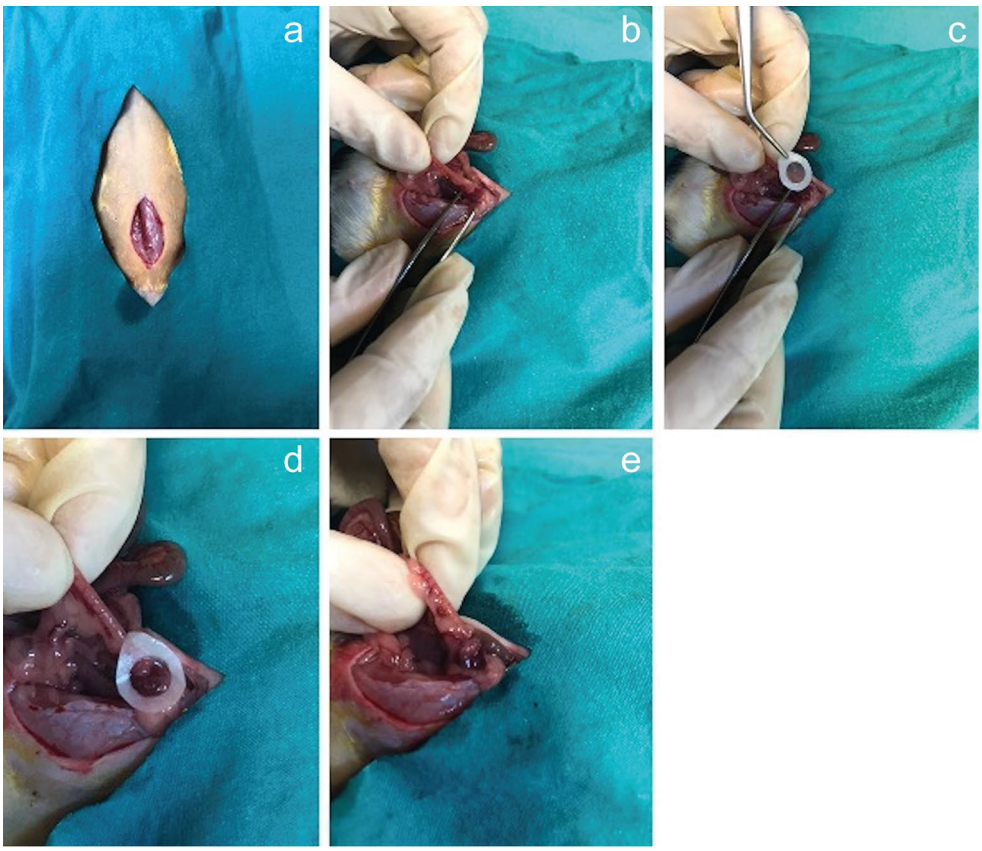


Fig. 3 **a** Cleaning the operation site with antiseptic solution with a midline incision being performed. **b** Right ovary was in the abdomen. **c** Cell sheet with tweezers. **d** Putting the cell sheet on the right ovary; taking away the protective layer of the cell sheet and wrapping the cell sheet on the right ovary. **e** Right ovary with cell sheet layer wrapped over it

Polyclonal Antibody, ref:bs-6612R, lot: YE1214W, USA); 1:200 [with PBS]; overnight at ±4 °C).

The density and intensity of the GDF-9 and BMP-15 stainings were evaluated in the ovary using a light microscope equipped with a digital camera (DM4000B Image Analyze System; Leica, Wetzlar, Germany), a Leica DFC280 plus camera and an LAS software program (Leica). We used the following semi-quantitative IHC scoring system to assess the GDF-9 and BMP-15 staining intensity: (0) no staining, (1) weak staining, (2) moderate to weak staining, (3) moderate staining, (4) moderate to strong staining, and (5) strong staining. Two independent observers, blind to the treatment protocol, evaluated the immunostaining scores separately. The *H* score was calculated as *H* score = ΣPi (*i* + 1), where the intensity of the GDF-9 and BMP-15 staining with values of 0–5, and Pi is the percentage of the stained cells for each "*I*"—intensity (Seymen et al. 2020).

TUNEL analysis

The sections were stained with an in-situ cell death detection kit (ApopTag Plus Peroxidase in Situ Apoptosis Detection Kit, Lot: PSO1514711, Chemicon International, Temecula, California, USA). Sections were evaluated on the LAS program by obtaining images with a Leica DM 4000 (Germany) computer-supported imaging system. Additionally, a negative control was performed, and the results were tested for immunohistochemical and TUNEL analyses (data not shown). The TUNEL index was calculated as a percentage of the TUNEL-positive nuclei among the total number of 100 counted nuclei.

RNA extraction, reverse transcription, and quantitative real-time PCR (qPCR) analysis

To evaluate the mRNA expression levels of the GDF-9 and BMP-15 genes, the entire RNA was extracted from the ovarian tissues using a TriReagent (peqGOLD TriFast™, peqlab, Germany), following the manufacturer's instructions. The RNA purity and concentration from each sample was determined using Nanodrop 100 spectrophotometry (Thermo Scientific, Waltham, MA). The RNA samples were stored at −80 °C until use. Reverse transcription (RT) was performed following the manufacturer's directions. Quantitative real-time polymerase chain reaction (qPCR) was conducted using a Transcriptor High Fidelity cDNA Synthesis Kit (Roche Diagnostics, Germany), in accordance performed for Gdf-9 and Bmp-15 mRNA levels using a Light Cycler 480 Probes Master mix (Roche Diagnostics GmbH) and analyzed using a Light-Cycler 480 instrument (Roche Diagnostics). Beta actin (Actb) was used as the housekeeping gene to normalize expression levels. The sequences of the gene-specific primers and universal probe library (UPL) numbers for Gdf-9, Bmp-15, and Actb are given in Table 1. Relative quantification of the mRNA levels was performed with the comparative Ct method using ΔΔCt with Actb as the reference gene and confirmed by the GeneGlobe Data Analysis Center (Qiagen) (Livak and Schmittgen 2001; Pfaffl et al. 2002). Each reaction was performed in triplicate.

Estradiol (E2) measurement

Venous blood samples were obtained by way of intracardiac puncture for analysis of the two parameters. The blood samples were centrifuged at 4000 rpm for 10 min and serum was removed and stored at −80 °C. Rat serum E2 (Cat No:202301/Lot No202207, SunRed Biotechnology Company,) analysis was performed by commercial Sandwich-ELISA kits. Both intra-CV and inter-CV were < 10%. The results are given as ng/L for E2.

Statistical analysis

All statistical analyses were performed by SPSS 25.0 software (IBM Corporation, Armonk, New York, USA). Statistical data were evaluated for normal distribution with a Shapiro-Wilk Francia test. The follicular count, E2 variables, PCR results, TUNEL, BMP-15, and GDF-9 quantitative variables of the groups were compared with a Kruskal–Wallis *H* test, and the results of the Monte Carlo simulation results. For the post hoc analysis, a Dunn's test was applied. Quantitative variables are shown in tables as median (minimum-maximum). The statistical data was examined at a 95% confidence interval and *p*-values less than 0.05 were statistically significant.

Table 1 Gene-specific primer sequences and UPL probe numbers

Gene	Forward primer	Reverse primer	UPL prob number
Bmp-15	5′-GCAATGAGGCTTCTCAGAGGT-3′	5′-AGTTGATGGCGGTAGACCA-3′	21
Gdf-9	5′-ATACCGTCCGGCTCTTCAG-3′	5'-TTAAATAGCAGGTCCACCATTG-3′	3
Actb	5′-CCCGCGAGTACAACCTTCT-3′	5′-CGTCATCCATGGCGAACT-3′	17

UPL universal probe library

Results

Immunofluorescent staining

Immunofluorescence staining photographs of the cell sheets are shown in Fig. 1a. The nuclei of the cells are marked in blue, and the F-actin filaments are marked in green, as seen in the photographs. Intense DAPI staining shows that the cells are overproliferated in the sheets. F-actin staining shows the orientation of the cytoskeleton within the sheets, and it is specified that the cells sheet contraction results in random and multidirectional orientation (Bou-Ghannam et al. 2021).

Live/dead cell staining

In the analysis, performed to determine the viability of the cells in the cell sheets, the cytoplasms of the living cells are seen in green and the nuclei of the dead cells are seen in red. Calcein AM transforms into calcein with esterase activity in living cells and gives a green fluorescence. On the other hand, Ethidium homodimer binds to nucleic acids and gives a red fluorescence because of disruption of membrane integrity in dead cells (Sokolowska et al. 2022). When the photographs were examined, it was determined that the cells preserved high vitality in the sheet. The dead cell nucleus is indicated by the red arrow (Fig. 1b).

Scanning electron microscopy (SEM) analysis

SEM images that display the morphological features of the produced cell sheets are given in Fig. 1c. The photographs show that the cell sheet is composed of multiple cell sheets and an intense and uniform ECM structure can be seen, as Zhou et al. observed in their study (Zhou et al. 2020). When the images are examined in detail, the close interactions of the cells with each other are observed. The collagen fibrils produced by the cells are shown with arrows in higher magnification.

BrdU staining results

As expected, the control group and POI group did not have BrdU staining. In the POI + IV AdMSCs and POI+ cell sheet groups staining was apparent. In all the ovarian sections, BrdU staining was more significant in the POI+ cell sheet group than in the POI + IV AdMSCs group. From this point, cell sheet application was more effective than applying AdMSCs by way of the IV method. In both groups, the AdMSCs settled in the stoma of the ovary. This

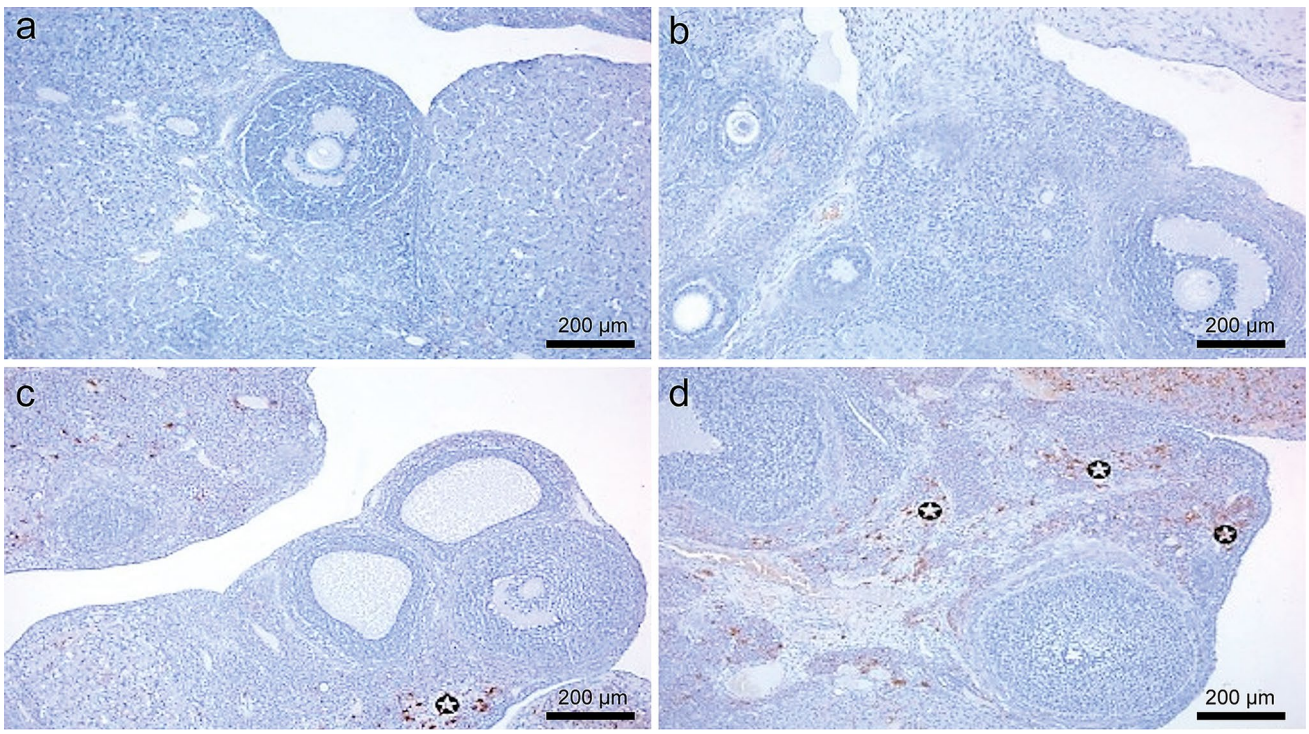


Fig. 4 Showing AdMSCs with BrdU staining. **a** control group. **b** POI group. **c** POI + IV AdMSC. **d** POI + cell sheet. Wingdings (✪), BrdU positive cells (Brdu-H ×100)

result supports the hypothesis that the AdMSCs activate foliculogenesis in a paracrine way (Fig. 4).

Hematoxylin-eosin results

In the control group, like normal ovarian tissue, there were follicles in different follicular stages in the cortex of the ovary. The medulla consisted of connective tissue with blood vessels. In higher magnification, there were primordial follicles surrounded by a single layer of squamous follicle cells, preantral follicles whose zona pellucida layer was clear, and atretic follicles which were similar with physiologic development.

In the POI group, dilated blood vessels were noticeable. In addition to this, there were significant atretic changes in the antral and Graafian follicles. There was also significant perifollicular fibrosis. The follicular shape was disturbed in Graafian follicles. There was also invasion of the fibrosis in the granulosa layer and a fibrotic theca structure in the follicular layer (Fig. 5a, b).

In the POI group treated by way of IV AdMSCs, follicles were seen in several developmental stages. Vascular dilatation and fibrosis were also obvious in this group. Although primordial and preantral follicles were seen in normal histomorphology, in certain antral follicles, there was duplication in the zona pellucida and edema in the granulosa cells. The most important finding in this group was antral follicles with multiple oocytes. The histomorphology of the Graafian follicles was similar with follicles in the POI group. In this group, a number of Graafian follicles were similar to PCOS as a large antrum and thinned granulosa layer (Fig. 5c).

In the POI group, treated by way of a cell sheet, follicles in several developmental stages were like the control group; however, edema and congestion in the medulla were remarkable. Different from the IV AdMSCs group and the POI

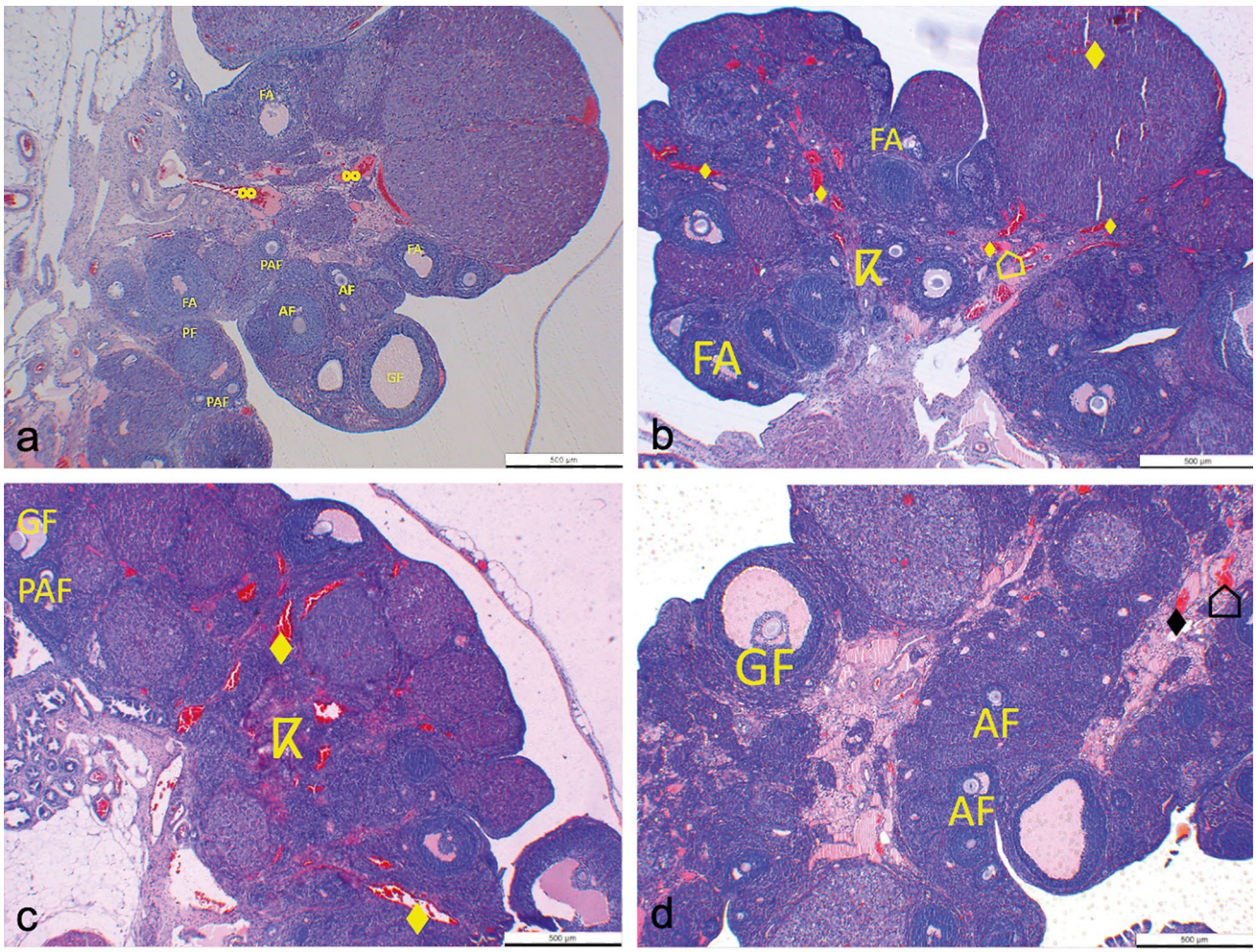


Fig. 5 Hematoxylin-eosin results of the following: **a** control group, **b** POI group, **c** POI + IV AdMSCs group, and **d** POI + CS group. Primoridal follicle, PF; preantral follicle, PAF; antral follicle, AF; Graaf follicle, GF; follicular atresia, FA; blood vessels; (∞), infinity; congestion in medullary blood vessels; (⌓), dilatation in blood vessels; (♦), black diamond suit; fibrosis in perifollicular area; Tifinagh letter yak (ⵅ) (H.E×40)

group, there were no follicles with morphological abnormality and fibrotic stroma (Fig. 5d).

Follicular count

There was statistical difference between the preantral follicle, antral follicle, and Graafian follicle count between the POI group and the other groups ($p < 0.05$). There was also a statistical difference between the preantral follicle count of the POI + IV AdMSCs group and the control group ($p = 0.014$). However, the preantral follicle count of the control group and the POI + CS groups were similar ($p > 0.05$). Atretic follicles were mostly seen in the POI group. The second group most noticeable for atretic follicles was the POI + IV AdMSCs group. There was no statistical difference between the control group and the POI + CS group ($p > 0.05$) (Fig. 6).

GDF-9 and BMP-15 immunostaining and H score results

GDF-9 protein defines the stage of preantral to antral transition in folliculogenesis. From this point of view, if it was compared to the control group, in the POI group entire follicles had weak immunoreactivity. In addition, in the POI + CS group, GDF-9 immunoreactivity was like the control group. With the POI + IV AdMSCs group, in several antral follicles, multiple oocytes were noticeable. There was weak immunostaining for GDF-9 in granulosa cells (Fig. 7). For more quantitative evaluation, an *H* score was calculated. The highest *H* score was in the control group and the lowest calculated in the POI group. In the POI + CS group, the GDF-9 *H* score was higher than in the POI + IV AdMSCs group. However, this difference was not statistically significant (Table 2).

BMP-15 describes the stage of antral to Graafian follicle transformation of folliculogenesis. In the POI group, immunostaining was weak. In the POI + IV AdMSCs group, BMP-15 immunostaining was weak compared to the control group, particularly in the granulosa cell layer. However, in the POI + CS group, the BMP-15 immunostaining was comparable to the control group (Fig. 8). For the *H* score, the lowest was the POI group and the highest was the control group (Table 2).

TUNEL results

Among the groups, the highest apoptosis was detected in the POI group. The atretic follicles were mostly antral, Graafian follicles, and granulosa and theca interna cells. In the POI + IV AdMSCs group, although the atretic follicle

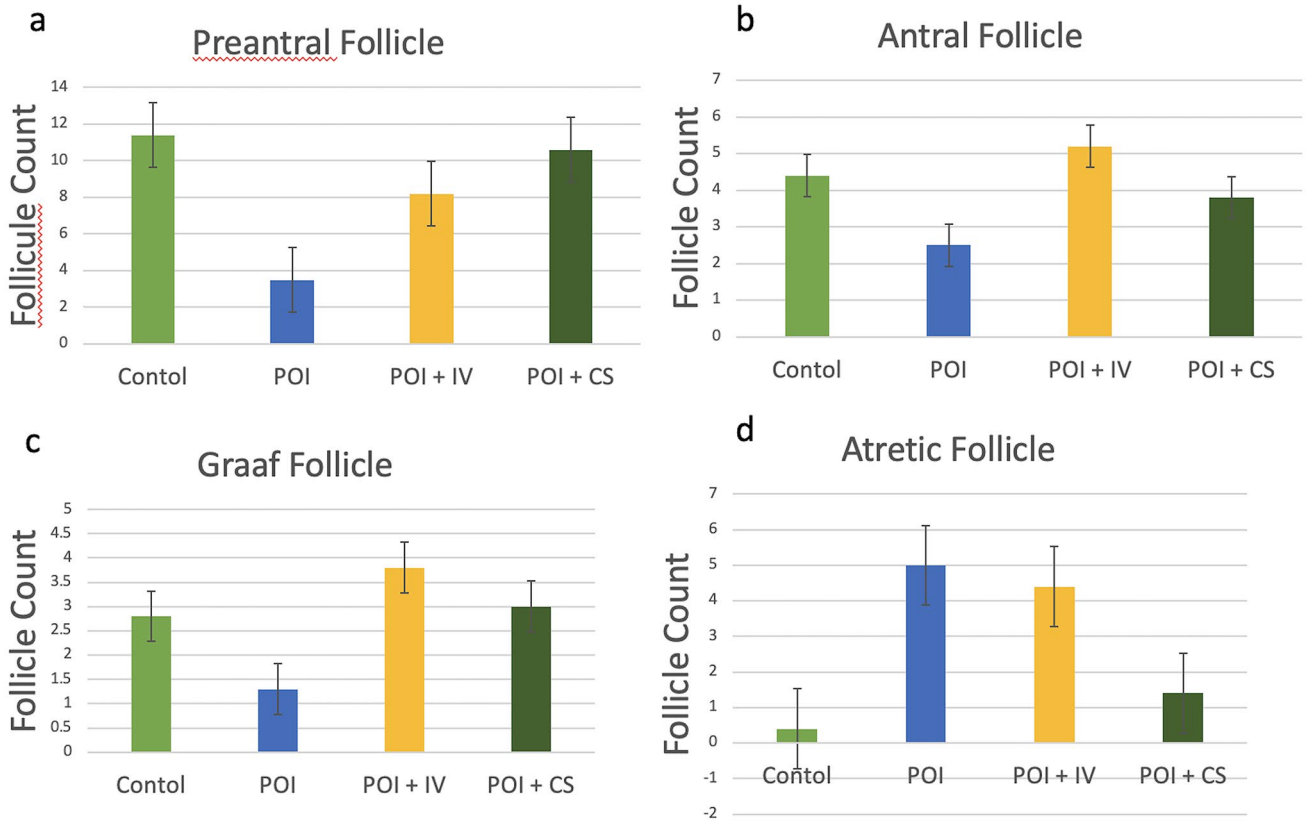


Fig. 6 Follicle counts of preantral, antral, Graafian, and atretic follicles in all the groups. *$p < 0.05$ compared to control, **$p < 0.05$ compared to POI, ***$p < 0.05$ compared to POI + CS

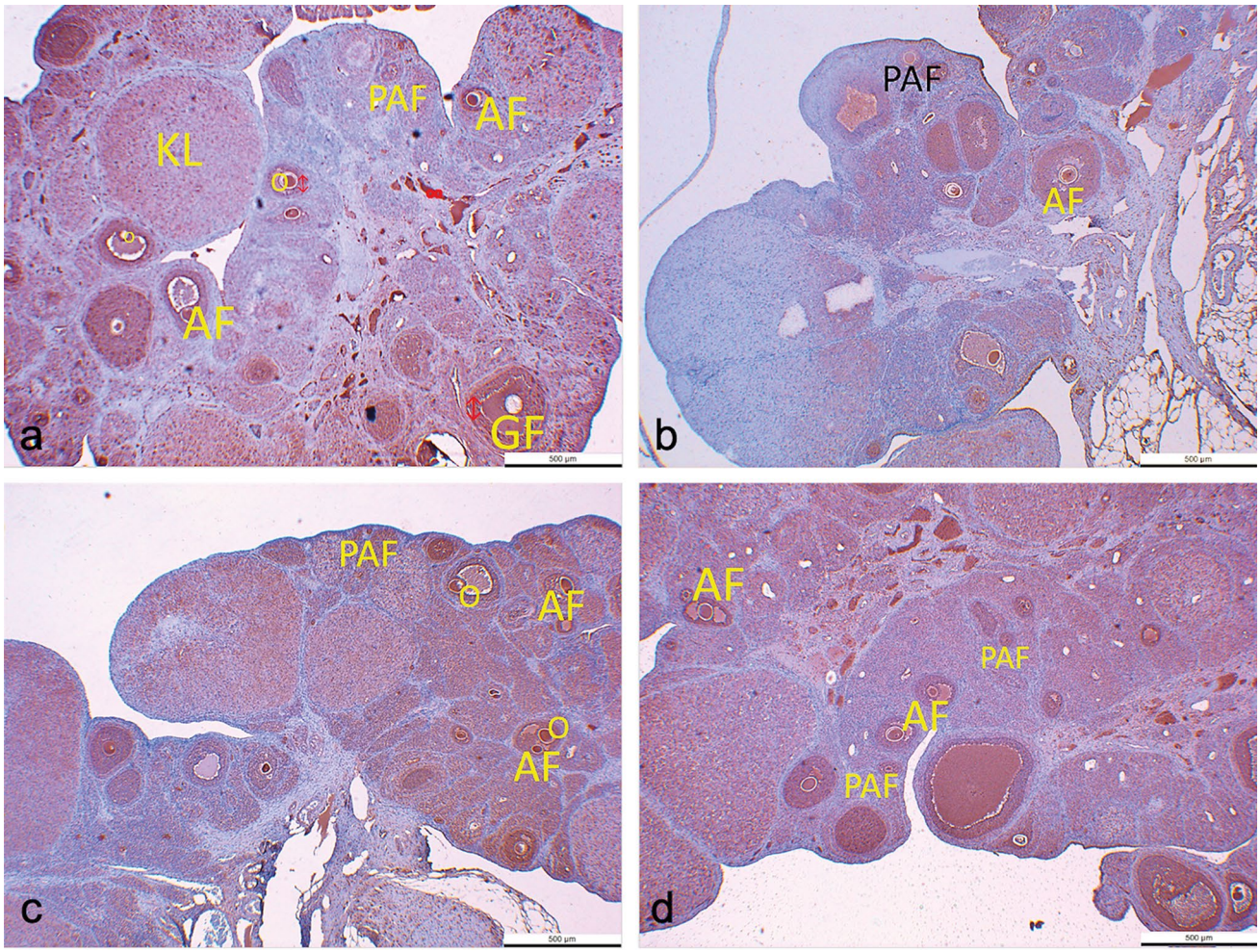


Fig. 7 GDF-9 immunostaining of the following: **a** control group, **b** POI group, **c** POI + IV AdMSCs group, and **d** POI + CS group. Preantral, PAF; antral follicle, AF; Graaf follicle, GF; corpus luteum, KL; oocyte, O; granulosa layer, ↕ (immunperoxidase hematoxylin ×40)

number decreased, apoptosis in the theca interna cells continued. On the other hand, in the POI + CS group, the atretic follicle count was similar to the control group (Fig. 9).

Gene expression results

The mRNAs expressions of the GDF-9 and BMP-15 genes were significantly less in the POI group compared to the control group ($p < 0.05$). On the other hand, in the POI + IV MSC and POI + CS groups, the mRNA expression levels were significantly higher than the experimental POI group ($p < 0.05$). However, the highest mRNA expression level of GDF-9 and BMP-15 was in the POI + CS group ($p < 0.05$) (Fig. 10).

E2 results

In the POI group, the E2 levels were lowest. Although the E2 levels were statistically significantly higher in the POI + IV AdMSCs group compared to the POI group ($p = 0.005$), the E2 levels of the POI + CS group were higher than the IV AdMSCs group but did not reach statistical significance ($p = 0.624$) (Table 2).

Discussion

In this study, our main hypothesis was that ovarian regeneration with the cell sheet method would be better than the IV method, without traumatizing the ovaries and applying stem cells to the systemic circulation. As a result, both intravenous AdMSCs administration and the cell sheet treatment approaches increased the follicle count and the GDF-9 and BMP-15 immunostaining and E2 levels compared to the POI group. In the IV approach, in contrast to the CS approach, atypical follicles (multioocytes) were detected. On the other hand, although it was not statistically significant, in the CS approach, the follicle count, E2 levels, and *H* score of immunostaining were higher than with the IV approach.

Table 2 The *H* scores of BMP-15 and GDF-9 immunostaining of follicles and estradiol values as well as the statistical significance for all the groups

	Estradiol	BMP15			GDF9		
		Preantral follicle	Antral Follicle	Graaf Follicle	Preantral follicle	Antral Follicle	Graaf Follicle
Groups	**Med. (min–max)**	**Med. (min-max)**	**Med. (min-max)**	**Med. (min-max)**	**Med. (min-max)**	**Med. (min-max)**	**Med. (min-max)**
Control ($n=5$)	158.5 (139.27–333.88)	2 (1–3)	2 (1–3)	2 (1–3)	3 (1–3)	2 (1–3)	2 (0.50–2)
POY ($n=4$)	51.77 (11.96–70.81)	1 (1–1)	1 (0–1)	1 (0–1)	1 (1–1)	1 (1–1)	0.25 (0–1)
IV ($n=4$)	96.17 (53.88–138.5)	1.50 (1–2)	2 (2–2)	2 (2–3)	2.50 (2–3)	2 (2–2)	2 (2–3)
CS ($n=4$)	101.58 (50.81–350.04)	2 (2–3)	2.50 (2–3)	3 (2–3)	3 (2–3)	2.50 (2–3)	2 (2–3)
***P* value**	**0.021**	**0.024**	**0.006**	**0.014**	**0.017**	**0.012**	**0.001**
Control vs POI	**0.005**	**0.015**	0.068	0.065	**0.022**	**0.016**	0.083
Control vs IV	0.063	0.191	0.635	0.716	0.924	0.726	0.203
Control vs CS	0.179	0.836	0.178	0.224	0.567	0.545	0.203
POI vs IV	0.363	0.290	**0.029**	**0.036**	**0.024**	**0.049**	**0.004**
POI vs CS	0.161	**0.013**	**0.003**	**0.004**	**0.007**	**0.004**	**0.004**
IV vs CS	0.624	0.151	0.408	0.419	0.651	0.365	0.999

Bold values were $p<0.05$ which was statistically significant

Kruskal-Wallis *H* test (Monte Carlo); post hoc test; Dunn's test. *Med* median, *Min* minimum, *Max* maximum, *vs* versus, *POI* premature ovarian insufficiency, *IV* intravenous, *CS* cell sheet

POI, with its increasing incidence, has become a serious health problem. A total of 90% of cases are idiopathic, and as the childbearing age has been postponed above the age of 35 in recent times, the major problem in POI has become infertility. However, there has not been a promising treatment for infertility in POI. In routine clinical practice, ART is the leading option; however, with a depleting follicle count, its success rate is questionable. In the literature, there are recent promising studies proposing that stem cell therapies might be a new option in the treatment of POI infertility. In a recent study by Yoon et al., stem cells were applied by IV to POI mice, and it was shown that folliculogenesis was activated (Yoon et al. 2020). With IV, because given that stem cells come across with several other factors in the bloodstream before arriving at damaged tissue, they can differentiate and be lost in the bloodstream. In this way, the amount of stem cells that are applied are less than the amount that migrate to the damaged tissue (Fu et al. 2021). In addition, the side effects of stem cells that were given to the blood stream are not well known. On the other hand, in a study by Mohamed et al. bone marrow derived mesenchymal stem cells (BMSC) were applied directly to the ovary by intraovarian injection (Mohamed et al. 2018). However, for this, BMSCs can only be applied to a limited area of the ovarian stroma. In addition, by applying injection directly to the ovary blindly, ovarian damage could occur.

From this point of view, the current study is designed to use cell sheet technology. Cell sheet engineering is one of the most challenging bottom-up approaches for tissue engineering. This scaffold-free technology was first introduced by Okano and his team. Cells were detached from the tissue culture surface with their own microenvironment in sheet form. Therefore, cell sheets have many advantages, including the easy delivery of cells to the target tissue, obtaining thick tissue by stacking sheets together, supporting wound healing, suppression of fibrosis, and increasing blood vessel formation (Chang et al. 2021). Initially, cell sheets are only produced by using thermo-responsive tissue culture plates, but then different methods have been developed for cell sheet formation such as magnetic force, light-induced, the ion-induced cell detachment method, fibrin coated dishes, or ascorbic acid treatment (Kaynak Bayrak and Gumusderelioglu 2019). It is known in the literature that ascorbic acid (AA) enhances cell proliferation, avoids cell apoptosis, and acts as an antioxidant. The main purpose of using AA in cell sheet production is its capacity to promote the synthesis of ECM components, especially collagen. It has also been shown that cell sheets obtained with 100 µg/mL AA had the maximum thickness, collagen synthesis,

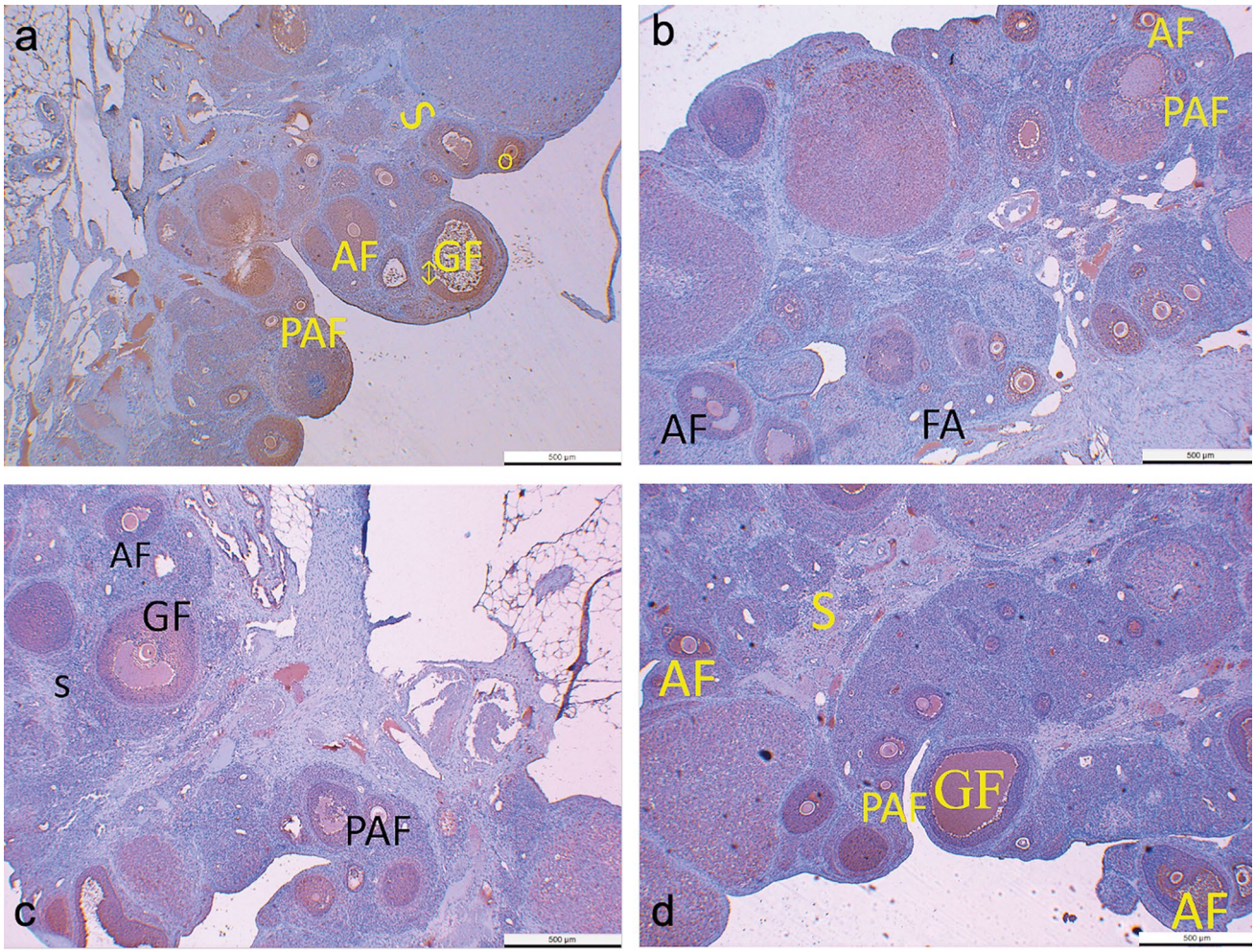


Fig. 8 BMP-15 immunostaining of the following: **a** control group, **b** POI group, **c** POI + IV AdMSCs group, and **d** POI + CS group. Preantral follicle, PAF; antral follicle, AF; Graaf follicle, GF; stroma, S; immunoreactivity in granulosa cells, ↕; oocyte, O; follicular atresia, FA (immunperoxidase hematoxylin ×40)

and the best mechanical strength (Kaynak Bayrak and Gumusderelioglu 2019; Shima et al. 2011). By considering this information, we decided to use 100 µg/mL AA for cell sheet production from ADMSCs in this study. With this new tissue engineering technology, in which stem cells can be used as a layer, stem cells can be applied directly to the ovary in an experimental POI model without harming tissue, and not applying stem cells to the blood stream. Cell sheets were successfully obtained on the fourth day of the culture. However, the cells were shanked upon detachment due to cytoskeletal contractile force between the cells and a loss of focal adhesion sites between the culture plate and the cells. As a result, the size of the cell sheets is smaller than the culture plate (Fig. 1d) (Nakao et al. 2019). Additionally, Bou-Ghannam et al. show that mesenchymal stem cells have a 3D morphology in the cell sheet after they detach from the surface and secrete more regenerative cytokines (Bou-Ghannam et al. 2021).

In addition to this, in one group, we applied AdMSCs by the IV method to compare efficiency with the cell sheet method. All the AdMSCs were marked with BrdU to prove the stem cell migration. Not only for the follicle count, but also to evaluate the folliculogenesis, GDF-9 and BMP-15 immunostaining and gene expressions of the proteins were also studied. Furthermore, to detect follicular function, E2 was studied from all the groups.

We used rats to generate the POI model parallel to the literature. In a recent study by Liu et al. (2014), BMSCs were applied to a cisplatin induced rat model. The study shows that the BMSCs migrated and prevented granulosa cell apoptosis (Liu et al. 2014). In another study by Besikcioglu et al. BMSCs were applied to the POI model and, after 30 days, E2, AMH, and FSH were compared only with the POI model (Besikcioglu et al. 2019). The E2 and AMH increased and the FSH decreased after stem cell application. In our study, in addition to these findings, prevention of granulosa cell

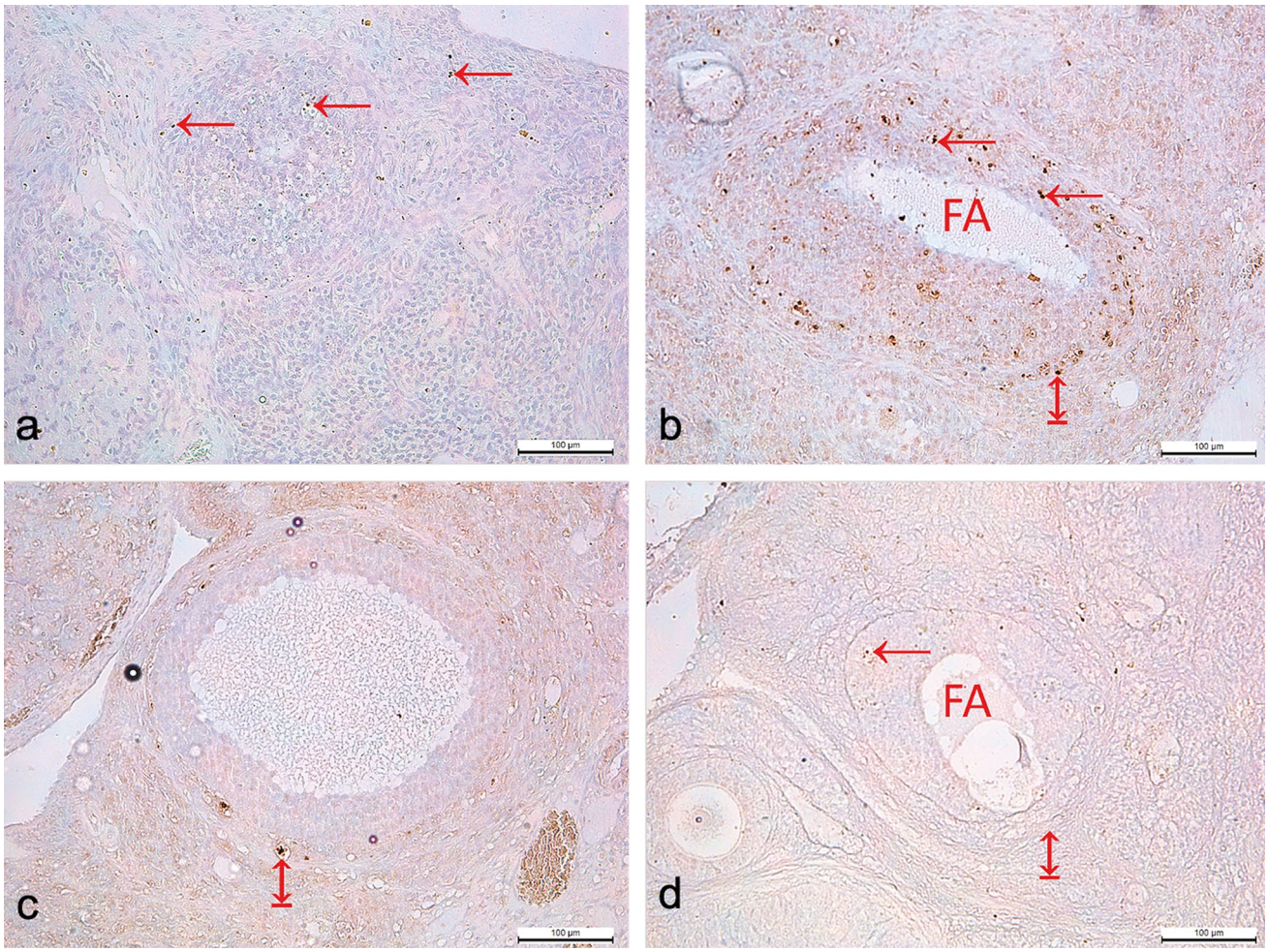


Fig. 9 **a** Control group TUNEL positive cells (←). **b** POI group TUNEL positive cells (←); follicular atresia, FA; positive theca interna cells(↕). **c** POI + IV AdMSCs group positive theca interna cells(↕). **d** POI + CS group TUNEL positive cells (←); (↕) (TUNEL-hematoxylin ×200)

apoptosis and E2 increase were shown in the IV group. However, in addition to the literature, in our study, AdMSCs were also applied by the cell sheet method. Compared to the IV method, the cell sheet prevented apoptosis of granulosa cells more and E2 recovery was distinct. In 2008, in a study by Mohamed et al. after MSC treatment in POI, induction of foliculogenesis was shown (Mohamed et al. 2018). In our study, we also evaluated the foliculogenesis steps by GDF-9 and BMP-15 immunostaining. Although foliculogenesis was induced in the stem cell groups compared to the POI group, in the CS group the antral follicle to the Graafian follicle improvement step in foliculogenesis was better induced than in the IV group, which was like the GDF-9 and BMP-15 gene expression results. Apart from this, in the current study, TUNEL immunostaining to show apoptosis was also examined. In the IV group, TUNEL immunostaining was established in theca interna cells, which can affect estrogen synthesis and affect implantation negatively. However, in the cell sheet group, TUNEL immunostaining was comparable to the control group, with no apoptosis in theca interna cells like the IV group. As a result, cell sheet treatment can support implantation in pregnancy compared to the IV group. In addition to this, for the atretic follicle count, there was a statistically significant difference between the IV and the cell sheet group.

In the current study, like the literature, AdMSCs were used for treatment (Ling et al. 2019; Vural et al. 2019). AdMSCs are obtained and produced easily, can be used as autolog or allogenic, and have a high capacity of differentiation. In addition to this, compared to the bone marrow aspiration for BMSC, obtaining adipose tissue has less morbidity. Apart from this, in a single liposuction, a larger amount of stem cells could be obtained compared to bone marrow aspiration.

Apart from that, in 2021, Yoshino et al. produced germ cell like cells from mouse pluripotent stem cells in vitro

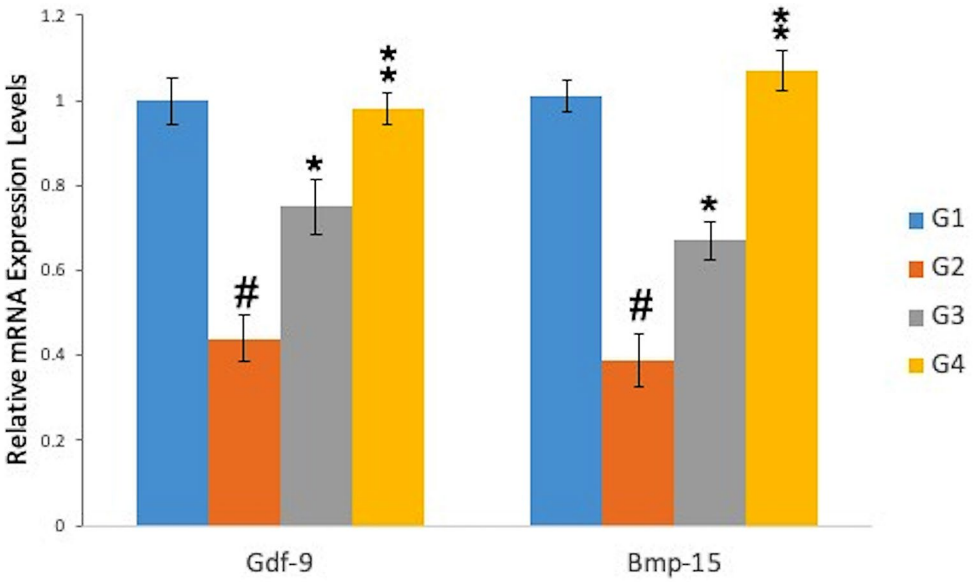


Fig. 10 The mRNA levels of the Gdf-9 and Bmp-15 genes were examined using qPCR analysis. The expression levels of the target genes were normalized to Actb mRNA levels as an internal control. $^{\#}p < 0.05$ compared with the control group. mRNA $^{*}p < 0.05$ compared with the G2 group. $^{**}p < 0.01$ compared with the G2 group. Actb, beta actin; qPCR, quantitative real-time PCR; mRNA, messenger RNA; PCR, polymerase chain reaction. G1, control group; G2, premature ovarian insufficiency group; G3, intravenous application group; G4, cell sheet group

(Yoshino et al. 2021). The main hypothesis of in vivo stem cell application is that given stem cells stimulate dormant follicles to restore folliculogenesis. However, in this study, functional oocytes can be formed from pluripotent stem cells. In this way, primordial germ cell-like cells can be produced without the need for in vivo stem cell application and ethical concerns, and pregnancy can be achieved with in vitro fertilization treatment. However, human pregnancy and live birth rates are still unknown in both methods (in vivo and in vitro). Future studies of both methods should be conducted to show which is better for POI patients.

This is a pioneering study that introduces the cell sheet method to the literature in the field of obstetrics and gynecology. By using this technology, without the administration of stem cells to systemic circulation and without traumatizing ovarian tissue by way of intraovarian injections, MSCs were applied all around the ovary homogenously. Strikingly, the results demonstrate that by AdMSCs sheet administration more regeneration is initiated and folliculogenesis is recovered better than with the IV method. In addition to this, although the same amount of stem cells was applied (4×10^5), both in the IV method and the cell sheet method, in the cell sheet method more stem cells were detected in the ovarian stroma than in the IV method. The main limitation of the current study is that, although the follicle count was analyzed in the experiment, the fecundability of the follicles was not studied. A second drawback is setting the trial on an animal model, and this cannot totally represent human results. In parallel with the literature (Bao et al. 2018) after applying MSCs as a cell sheet or IV method in our study, we sacrificed rats after 28 days to prove the effect of MSCs. After 28 days, we were able to see a significant difference in follicle count and foliculogenesis between the groups. However, as this is an animal study, it is not entirely representative of human data. In order to increase the efficiency of the cell sheet, in future studies the *tunica albuginea* in the ovary can be punched several times, then the cell sheet can be placed on top of the ovarian tissue. In this way, the migration of stem cells can be more towards the ovarian cortex under the *tunica albuginea.*

To develop future studies, recovered follicle viability and fecundability should also be investigated. Although the current study shows that the cell sheet method is better at preventing apoptosis, both in granulosa and theca cells as well as stimulating folliculogenesis, before extrapolating these results into clinical practice, the current findings should be confirmed with human data.

Acknowledgements The authors wish to thank the TSRM and TAJEV societies for their support.

Funding The study was awarded the "Best Research" award at the TSRM 2018 Congress and was also awarded the "Best Abstract" award at the TAJEV 2022 Congress. The study was funded by award money.

Data availability The data that supports the findings of this study are available on requests.

Declarations

Ethics approval All procedures involving animals followed the European Community Council Directive of 24 November 1986, and ethical approval was granted by the Gazi University Ethical Committee on Animal Research (Approval No: 21/12/2018-E.168939).

Conflict of interest The authors declare no competing interests.

References

Akdere OE, Shikhaliyeva I, Gumusderelioglu M (2019) Boron mediated 2D and 3D cultures of adipose derived mesenchymal stem cells. Cytotechnology 71:611–622

Bao R, Xu P, Wang Y, Wang J, Xiao L, Li G, Zhang C (2018) Bone marrow derived mesenchymal stem cells transplantation rescues premature ovarian insufficiency induced by chemotherapy. Gynecol Endocrinol 34:320–326

Besikcioglu HE, Saribas GS, Ozogul C, Tiryaki M, Kilic S, Pinarli FA, Gulbahar O (2019) Determination of the effects of bone marrow derived mesenchymal stem cells and ovarian stromal stem cells on follicular maturation in cyclophosphamide induced ovarian failure in rats. Taiwan J Obstet Gynecol 58:53–59

Bou-Ghannam S, Kim K, Grainger DW, Okano T (2021) 3D cell sheet structure augments mesenchymal stem cell cytokine production. Sci Rep 11:8170

Chang D, Fan T, Gao S, Jin Y, Zhang M, Ono M (2021) Application of mesenchymal stem cell sheet to treatment of ischemic heart disease. Stem Cell Res Ther 12:384

Chen G, Qi Y, Niu L, Di T, Zhong J, Fang T, Yan W (2015) Application of the cell sheet technique in tissue engineering. Biomed Rep 3:749–757

Diaz-Garcia C, Herraiz S, Pamplona L, Subira J, Soriano MJ, Simon C, Seli E, Pellicer A (2022) Follicular activation in women previously diagnosed with poor ovarian response: a randomized, controlled trial. Fertil Steril 117:747–755

Fu YX, Ji J, Shan F, Li J, Hu R (2021) Human mesenchymal stem cell treatment of premature ovarian failure: new challenges and opportunities. Stem Cell Res Ther 12:161

Kawamura K, Kawamura N, Hsueh AJ (2016) Activation of dormant follicles: a new treatment for premature ovarian failure? Curr Opin Obstet Gynecol 28:217–222

KaynakBayrak G, Gumusderelioglu M (2019) Construction of cardiomyoblast sheets for cardiac tissue repair: comparison of three different approaches. Cytotechnology 71:819–833

Li J, Mao Q, He J, She H, Zhang Z, Yin C (2017) Human umbilical cord mesenchymal stem cells improve the reserve function of perimenopausal ovary via a paracrine mechanism. Stem Cell Res Ther 8:55

Ling L, Feng X, Wei T, Wang Y, Wang Y, Wang Z, Tang D, Luo Y, Xiong Z (2019) Human amnion-derived mesenchymal stem cell (hAD-MSC) transplantation improves ovarian function in rats with premature ovarian insufficiency (POI) at least partly through a paracrine mechanism. Stem Cell Res Ther 10:46

Liu J, Zhang H, Zhang Y, Li N, Wen Y, Cao F, Ai H, Xue X (2014) Homing and restorative effects of bone marrow-derived mesenchymal stem cells on cisplatin injured ovaries in rats. Mol Cells 37:865–872

Livak KJ, Schmittgen TD (2001) Analysis of relative gene expression data using real-time quantitative PCR and the 2(-Delta Delta C(T)) method. Methods 25:402–408

Martin LA, Porter AG, Pelligrini VA, Schnatz PF, Jiang X, Kleinstreuer N, Hall JE, Verbiest S, Olmstead J, Fair R, Falorni A, Persani L, Rajkovic A, Mehta K, Nelson LM, Rachel's Well Primary Ovarian Insufficiency Community of Practice G (2017) A design thinking approach to primary ovarian insufficiency. Panminerva Med 59:15–32

Mohamed SA, Shalaby SM, Abdelaziz M, Brakta S, Hill WD, Ismail N, Al-Hendy A (2018) Human mesenchymal stem cells partially reverse infertility in chemotherapy-induced ovarian failure. Reprod Sci 25:51–63

Nakao M, Inanaga D, Nagase K, Kanazawa H (2019) Characteristic differences of cell sheets composed of mesenchymal stem cells with different tissue origins. Regen Ther 11:34–40

Nelson LM (2009) Clinical practice. Primary ovarian insufficiency. N Engl J Med 360:606–614

Owaki T, Shimizu T, Yamato M, Okano T (2014) Cell sheet engineering for regenerative medicine: current challenges and strategies. Biotechnol J 9:904–914

Pfaffl MW, Horgan GW, Dempfle L (2002) Relative expression software tool (REST) for group-wise comparison and statistical analysis of relative expression results in real-time PCR. Nucleic Acids Res 30:e36

Seymen CM, CakirGundogdu A, Bulut DI, Yilmaz Demirtas C, Elmas C (2020) Royal jelly increased map-2 expression in hippocampal neurons of hypothyroid rats: an immunohistochemical study. Biotech Histochem 95:46–54

Shima N, Kimoto M, Yamaguchi M, Yamagami S (2011) Increased proliferation and replicative lifespan of isolated human corneal endothelial cells with L-ascorbic acid 2-phosphate. Invest Ophthalmol Vis Sci 52:8711–8717

Shimizu T, Yamato M, Kikuchi A, Okano T (2003) Cell sheet engineering for myocardial tissue reconstruction. Biomaterials 24:2309–2316

Sokolowska P, Siatkowska M, Bialkowska K, Rosowski M, Komorowski P, Walkowiak B (2022) Osteosarcoma cells in early and late stages as cancer in vitro progression model for assessing the responsiveness of cells to silver nanoparticles. J Biomed Mater Res B Appl Biomater 110:1319–1334

Vural B, Duruksu G, Vural F, Gorguc M, Karaoz E (2019) Effects of VEGF (+) mesenchymal stem cells and platelet-rich plasma on inbred rat ovarian functions in cyclophosphamide-induced premature ovarian insufficiency model. Stem Cell Rev Rep 15:558–573

Wang S, Yu L, Sun M, Mu S, Wang C, Wang D, Yao Y (2013) The therapeutic potential of umbilical cord mesenchymal stem cells in mice premature ovarian failure. Biomed Res Int 2013:690491

Yilmaz MM, Akdere OE, Gumusderelioglu M, KaynakBayrak G, Koc S, Erdem A, Tuncer M, Atalay O, Take Kaplanoglu G, AkarcaDizakar SO, Calis M (2023) Biological nerve conduit model with de-epithelialized human amniotic membrane and adipose-derived mesenchymal stem cell sheet for repair of peripheral nerve defects. Cell Tissue Res 391:505–522

Yoon SY, Yoon JA, Park M, Shin EY, Jung S, Lee JE, Eum JH, Song H, Lee DR, Lee WS, Lyu SW (2020) Recovery of ovarian function by human embryonic stem cell-derived mesenchymal stem cells in cisplatin-induced premature ovarian failure in mice. Stem Cell Res Ther 11:255

Yoshino T, Suzuki T, Nagamatsu G, Yabukami H, Ikegaya M, Kishima M, Kita H, Imamura T, Nakashima K, Nishinakamura R, Tachibana M, Inoue M, Shima Y, Morohashi KI, Hayashi K (2021) Generation of ovarian follicles from mouse pluripotent stem cells. Science 373

Zhang Q, Bu S, Sun J, Xu M, Yao X, He K, Lai D (2017) Paracrine effects of human amniotic epithelial cells protect against chemotherapy-induced ovarian damage. Stem Cell Res Ther 8:270

Zhou S, Wang Y, Zhang K, Cao N, Yang R, Huang J, Zhao W, Rahman M, Liao H, Fu Q (2020) The fabrication and evaluation of a potential biomaterial produced with stem cell sheet technology for future regenerative medicine. Stem Cells Int 2020:9567362

Publisher's Note Springer Nature remains neutral with regard to jurisdictional claims in published maps and institutional affiliations.

Springer Nature or its licensor (e.g. a society or other partner) holds exclusive rights to this article under a publishing agreement with the author(s) or other rightsholder(s); author self-archiving of the accepted manuscript version of this article is solely governed by the terms of such publishing agreement and applicable law.